Reactions at oxide surfaces

1989 J. Phys.: Condens. Matter 1 SB111

(http://iopscience.iop.org/0953-8984/1/SB/019)

J. Phys.: Condens. Matter 1 (1989) SB111–SB117. Printed in the UK

Reactions at oxide surfaces

G Thornton
Interdisciplinary Research Centre in Surface Science and Chemistry Department, Manchester University, Manchester M13 9PL, UK

Received 24 April 1989

Abstract. This paper describes some recent studies of adsorbate interactions at oxide surfaces using photo-emission, surface EXAFS and NEXAFS which illustrate the potential of the techniques to provide structural and mechanistic information. The examples chosen are a SEXAFS study of the NiO(100)–H_2S reaction, which results in reduction of the substrate to form a Ni(100)c(2 × 2)S raft; a NEXAFS study of the thermally activated reaction of SO_2 with TiO_2(110) resulting in surface sulphate formation; and photo-emission work which evidences the dissociation of H_2O by $SrTiO_3$(100) catalytic step sites.

1. Introduction

Understanding oxide surface reactivity at the atomic level is one of the next major challenges in surface science. Although it is difficult to generalise about a class of materials with such diverse properties, a major difference between metal and oxide surface reactivity lies in the role of minority sites such as vacancies and steps. This can be understood by remembering that a metal ion at an oxide surface step site will have an associated electrostatic potential similar in many respects to that associated with a 'promoter' alkali metal atom adsorbed on a metal surface. Of course we expect other much more fundamental differences in the reactivity: for instance there is no metal surface counterpart to an oxide surface reduction reaction.

Thus far, there have been rather few single-crystal studies aimed at elucidating the detailed mechanism of oxide surface reactions, including the role of specific minority sites in the reactivity. These are detailed in recent review articles by Henrich [1] and Heiland and Lüth [2]. The approach we have adopted involves the study of model reactions using synchrotron radiation techniques, three examples of which are described below. The first is a surface-extended x-ray absorption fine structure (SEXAFS) study of H_2S adsorption on NiO(100), which at 570 K results in reduction of the substrate to form a Ni(100)c(2 × 2)S oriented raft. The second example consists of a near-edge x-ray absorption fine structure (NEXAFS) study of the SO_2–TiO_2(110) reaction. Here SO_2 adsorbed at 100 K reacts with the substrate at higher temperatures to form a stable surface sulphate species. The final example addresses minority site reactivity, where we have investigated the role of step and point defects (oxygen vacancies) in the reaction of $SrTiO_3$(100) with H_2O using photo-emission spectroscopies. We find that step sites catalytically dissociate H_2O while point defects play only a secondary role in the reaction [3].

0953-8984/89/SB0111 + 07 $02.50

2. Experimental

Photo-emission and x-ray absorption measurements were carried out using a double-pass cylindrical mirror analyser (CMA) (Physical Electronics Inc.) on stations 6.1 ($30\,eV \leqslant h\nu \leqslant 200\,eV$) and 6.3 ($1800\,eV \leqslant h\nu \leqslant 11000\,eV$) at the SRS, Daresbury Laboratory. In the $SrTiO_3(100)$ study the combined energy resolution (monochromator + analyser) was ~1.0 and 0.4 eV (full width at half maximum, FWHM) at photon energies of 180 and 110 eV respectively. In the SEXAFS and NEXAFS work the CMA was used to record the yield of S KLL Auger electrons (kinetic energy = 2100 eV) as a monitor of the surface absorption coefficient above the S K edge (2472 eV). Using the Auger yield method necessarily limits the data range to about 150 eV above the S K edge, because at this photon energy the substrate O 1s photo-electron peak enters the analyser energy window. Normalisation to the incident x-ray flux was accomplished by measuring the drain current from a thin Al foil placed between the monochromator and the sample.

Fracturing n-type $SrTiO_3$ parallel to the (100) planes *in situ* at a chamber pressure of $\leqslant 8 \times 10^{-11}$ mbar yielded a stepped unreconstructed (100) face as determined by low-energy electron diffraction (LEED). The planar surface was prepared by Ar^+ bombardment and annealing in oxygen, yielding a clean unreconstructed surface as measured by Auger and LEED. For the fractured surface, exposure to H_2O vapour and subsequent measurements were carried out at 300 K. Because planar $SrTiO_3(100)$ does not react with H_2O at room temperature, exposure and measurements were performed at a sample temperature of 150 K. No noticeable change in the LEED patterns was observed following exposure to H_2O, indicating the formation of disordered overlayers. The clean $TiO_2(110)$ surface was prepared by Ar^+ bombardment and annealing in oxygen, with the ~200 L (1 Langmuir = 1.32×10^{-6} mbar s) SO_2 exposure carried out at 100 K. The 1×1 LEED pattern of the clean surface was extinguished on exposure, probably because of SO_2 multi-layer formation. A clean NiO(100)1×1 surface was prepared by cleaving *in situ*. Exposure to 2×10^4 L of H_2S was carried out with the sample at 570 K [4], the measurements being performed at 155 K.

3. Results and discussion

3.1. NiO(100) + H_2S

In previous work the LEED pattern obtained after reacting NiO(100) with H_2S at 570 K was interpreted on the basis of Ni(100)c(2×2)S overlayer formation [4]. In this model the overlayer is azimuthally aligned with the substrate, as indicated in figure 1(*a*). In the present work we sought to test this idea using S K edge SEXAFS; the χk^2 spectrum recorded at normal incidence and its Fourier transform is shown in figure 1(*b*).

Analysis of the EXAFS spectrum using a curve-fitting routine based on the rapid curved wave computational scheme [5] gave a nearest-neighbour S–Ni bond distance of 2.26 ± 0.04 Å (using a 0.06 Å correction to the theoretical phase shift [6]) and an effective coordination number of 3.8 ± 1.5. Both the bond distance and the coordination number results are consistent with those expected for S in the four-fold hollow of a Ni(100) plane [6]. This, along with the rejection by the analysis routine of an oxygen backscattering atom, strongly supports the Ni(100)c(2×2) raft model.

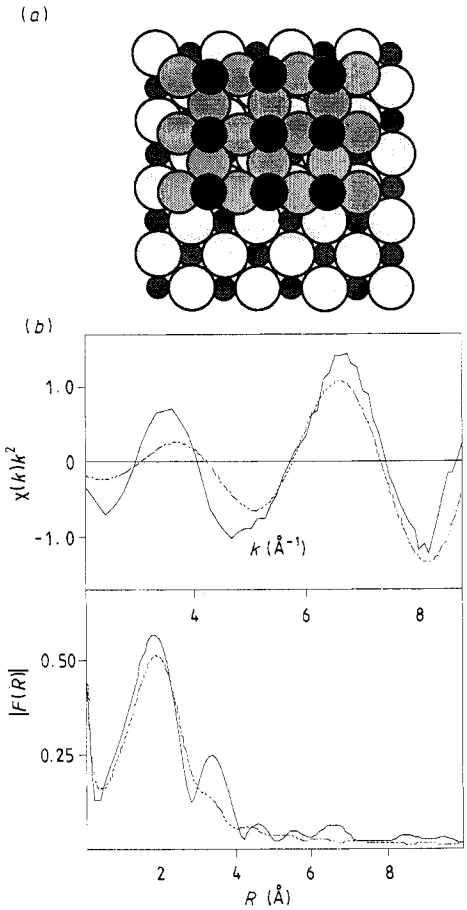

Figure 1. (*a*) The structural model derived from the LEED pattern [4]. In this model substrate Ni atoms are represented by the small shaded circles, O atoms by the open circles. Ni atoms in the Ni(100) plane are shaded and S atoms are black. (*b*) S KLL Auger yield SEXAFS spectra of NiO(100) following H_2S adsorption at 570 K and cooling to 155 K, recorded at normal incidence. The EXAFS function $\chi(k)$ weighted by k^2 (full curve) and the best theoretical fit (broken curve) are compared in the upper part of the figure. The lower section contains the modulus of the Fourier transform.

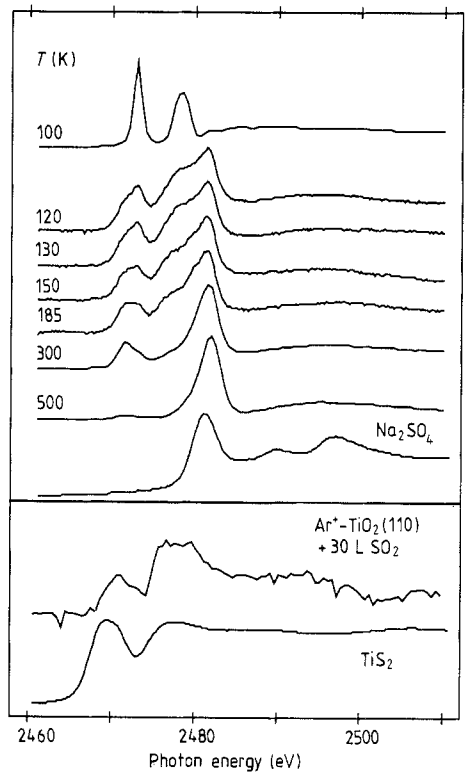

Figure 2. S KLL Auger yield NEXAFS spectra of TiO_2(110) following SO_2 adsorption at 100 K and annealing to the indicated temperatures. All measurements were recorded at ~100 K and at 70° angle of incidence. Also shown is a spectrum recorded following 300 K adsorption of SO_2 on the Ar^+ bombarded surface, as well as fluorescence yield NEXAFS spectra of TiS_2 and Na_2SO_4. The latter spectra were recorded using station 3.4 at the SRS.

3.2. TiO_2(110) + SO_2

Previous work on this system is restricted to a room temperature adsorption study using UV and x-ray photoemission (UPS, XPS) and LEED. Smith *et al* [7] found essentially no reaction with the nearly perfect surface and formation of a surface sulphide phase when SO_2 is reacted with a defected surface created by Ar^+ bombardment.

In contrast to the earlier work, we have concentrated on lower-temperature adsorption and the effect of thermal activation. The S K edge NEXAFS spectra are shown in

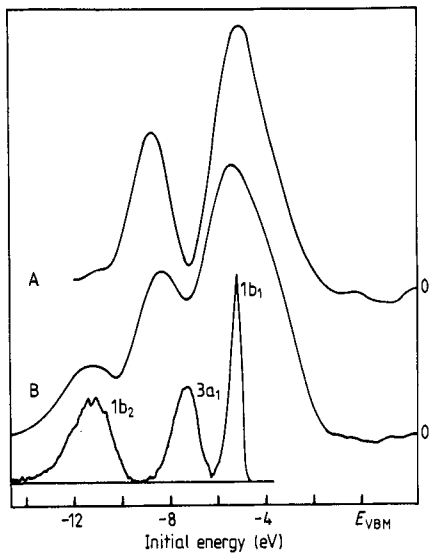

Figure 3. UPS difference spectra (H_2O-clean) for: A, 10 L H_2O on stepped $SrTiO_3(100)$ adsorbed at 300 K; B, 0.5 L H_2O on planar $SrTiO_3(100)$ adsorbed at 150 K (with $h\nu$ = 140 eV), compared with C, a gas-phase photo-electron spectrum of H_2O from [10], aligned at the $1b_2$ energy ($h\nu$ = 28.4 eV).

figure 2. Condensing SO_2 at 100 K gives rise to NEXAFS identical to that obtained in the gas phase spectrum, from which the two major features observed have been assigned to S 1s$\rightarrow \pi^*$ (2473 eV) and σ^* (2478 eV) resonances [8]. On annealing the sample incrementally, the SO_2 features decrease in intensity and appear to be replaced by similar peaks shifted to 1 eV lower photon energy and a new resonance at 2482 eV. At higher anneal temperatures the 'shifted SO_2 features' decrease in intensity leaving the 2482 eV resonance. For comparison with the earlier photo-emission work [7] we also show in figure 2 a room temperature spectrum recorded after Ar^+ bombardment and exposure to 30 L of SO_2.

The maintenance of the 2473 eV and 2478 eV features probably arises from re-adsorption of SO_2 at 100 K to form multi-layer islands. The most obvious assignment of the shifted peaks would be to a chemisorbed SO_2 species having longer S–O bond distances than molecular SO_2. While additional work is needed to clarify these points, it is tempting to speculate that it could represent an intermediate between the initial adsorption phase and formation of a surface sulphate. The latter is indicated by the presence of the 2482 eV resonance, which is characteristic of a SO_4^{2-} species [9] (see figure 2).

In that the NEXAFS spectrum obtained from the Ar^+ bombarded surface is similar to that obtained from TiS_2 (see figure 2) our results of this surface are consistent with the conclusions of Smith *et al* [7]. The surface spectrum is somewhat broader, which probably reflects the variety of surface sites available on the Ar^+ bombarded surface, and hence the variety of surface sulphide and possibly other micro-phases formed.

3.3. $SrTiO_3(100) + H_2O$

A comparison of valence band photo-emission spectra obtained from the stepped and planar (100) surfaces before and after exposure to H_2O is shown in figure 3 in the form of difference spectra. These data indicate that the mode of adsorption is different for the two surfaces, being molecular in the case of the planar surface (at <200 K) and dissociative on the stepped surface, where the initial sticking coefficient is close to unity.

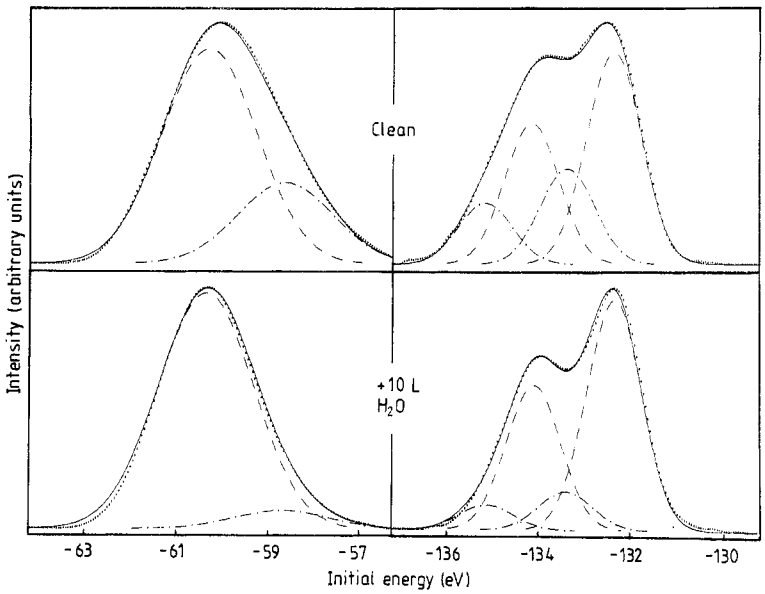

Figure 4. Ti 3s (left panel) and Sr 3d (right panel) photo-emission spectra of clean and H_2O dosed stepped $SrTiO_3(100)$, recorded at $h\nu$ = 110 eV (Ti 3s) and $h\nu$ = 180 eV (Sr 3d). The spectra have been background subtracted and fitted to symmetric gaussian peaks. Initial energy is referenced to the valence band maximum. Both the bulk and surface Sr 3d features are spin–orbit split by ~1.8 eV. - - - - bulk; – · – · – surface; —— total; · · · · experiment.

In order to learn more about the adsorption mechanism, it is helpful to have a direct probe of the substrate atoms. This is provided by surface core level chemical shifts (SCLS) in the 'surface sensitive' XPS spectrum made possible by the use of a tunable photon source. Sr 3d and Ti 3s core level spectra of the stepped surface are shown in figure 4, along with spectra recorded after H_2O adsorption. The photon energies used yield Sr 3d and Ti 3s photo electron kinetic energies of ~40 eV, corresponding to an electron mean free path of ~7 Å [11]. Similar spectra are obtained from the planar surface, in that the same SCLS features are present, although at different relative intensities. From the former observation we can deduce that the SCLS features arise from Sr and Ti atoms on terrace sites. Having the simple-cubic perovskite structure, $SrTiO_3(100)$ contains two types of crystal plane parallel to (100), one of which contains Sr and O atoms (SrO-type), the other containing Ti and O atoms (TiO_2-type). Hence the SCLS features in figure 4 arise from cations on their respective terraces. Whereas on the stepped surface the Sr and Ti surface to bulk ratios are equal as expected, different ratios are possible on the planar surface depending on the details of preparation. The SCLS value obtained for Sr (-1.00 ± 0.05 eV) compares sensibly with the value calculated by Wolfram *et al* [12] of -1.23 eV, although this neglects surface relaxation and final state effects. The measured Ti value (1.7 ± 0.1 eV), however, is in marked disagreement with that calculated (-2.0 eV), which most obviously arises from a surface enhanced covalency effect not included in the calculations [13].

Both the Sr and Ti SCLS seen in figure 4 are attenuated on H_2O adsorption, suggesting the formation of Ti–OH and Sr–OH species, where the cation potentials would be similar to the bulk values, with H atoms bound to O terrace sites. In contrast only the Sr SCLS feature in the planar surface spectrum is attenuated on adsorption.

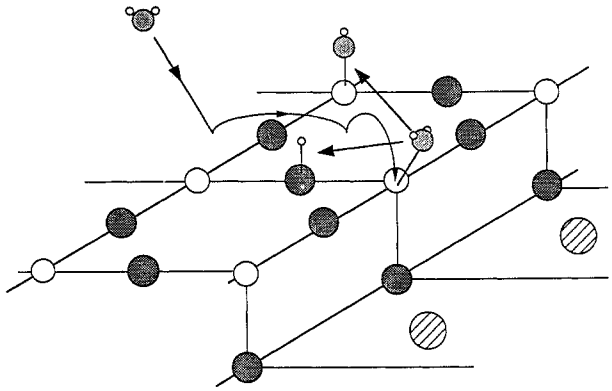

Figure 5. A schematic model of H_2O adsorption on the stepped $SrTiO_3(100)$ surface. O atoms are shown as full circles; Ti atoms as open circles; and Sr atoms as hatched circles.

By reference to only the valence band spectra we might reasonably have proposed that steps activate H_2O dissociation. However, the SCLS data allow us to exclude the possibility that active sites are located on a (100) terrace type not present on the planar surface. Another possible source of active sites are oxygen vacancies created in sample preparation, although this can be excluded on the grounds that the stepped and planar surfaces have a similar concentration, as estimated from their characteristic band gap state. We therefore conclude that the steps are the active sites for H_2O dissociation. From the initial sticking coefficient and SCLS data we deduce a mechanism of H_2O adsorption on the stepped surface shown schematically in figure 5. This involves diffusion of H_2O across terraces to steps, the dissociation products subsequently migrating back to terrace sites. Hence the step sites are renewable and are acting as true catalytic centres. In seeking an explanation for the enhanced reactivity of step sites, it seems more likely that the low-coordination Ti sites are reactive, since here the 3d orbital occupation will be maximised. Following the ideas of Kowalski *et al* [14], the O–H_2 bonds would be weakened by interaction of occupied 3d orbitals with H_2O antibonding orbitals.

4. Conclusions

This paper has outlined the study of three oxide surface reactions, chosen to illustrate the diversity of the surface science involved, and the potential of synchrotron radiation techniques in its study. In many ways the studies pose more questions than they answer; for instance, is the Ni(100)c(2 × 2)S overlayer formed in the NiO(100)–H_2S reaction buckled to accommodate the undulating NiO substrate? This type of question can in principle be answered using SEXAFS and forms part of our programme of future research.

Acknowledgments

This work, which was funded by the SERC (UK), involved a collaboration with C A Muryn, D Purdie, N B Brookes, N S Prakash, A L Johnson, D R Warbuton, F M Quinn and D S-L Law.

References

[1] Henrich V E 1988 *Surface and Near-Surface Chemistry of Oxide Materials* ed J Nowotny and L-C Dufour (Amsterdam: Elsevier) pp 23–60
1985 *Rep. Prog. Phys.* **48** 1481–1541
[2] Heiland G and Lüth H 1984 *The Chemical Physics of Solid Surfaces and Heterogenous Catalysis* ed D A King and D P Woodruff, vol 3b (Amsterdam: Elsevier) pp 137–223
[3] Brookes N B, Quinn F M and Thornton G 1987 *Solid State Commun.* **64** 383–6
[4] Steinbrunn A, Dumas P and Colson J C 1978 *Surf. Sci.* **74** 201–15
[5] Gurman S J, Binsted N and Ross I 1984 *J. Phys. C: Solid State Phys.* **17** 143–51
[6] Brennan S, Stöhr J and Jaeger R 1981 *Phys. Rev.* B **24** 4871–4
[7] Smith K E, MacKay J L and Henrich V E 1987 *Phys. Rev.* B **35** 5822–9
[8] Bodeur S and Esteva J M 1985 *Chem. Phys.* **100** 415–27
[9] Sekiyama H, Kosugi N, Kuroda H and Ohta T 1986 *Bull. Chem. Soc. Japan* **59** 575–9
[10] Truesdale C M, Southworth S H, Kobrin P H, Lindle D W, Thornton G and Shirley D A 1982 *J. Chem. Phys.* **76** 860–5
[11] Seah M P and Dench W A 1979 *Surf. Interface Analysis* **1** 2
[12] Kraut E A, Wolfram T and Hall W 1972 *Phys. Rev.* B **6** 1499–1503
[13] Wolfram T and Ellialtioglu S 1977 *Appl. Phys.* **13** 21–4
[14] Kowalski J M, Johnson K H and Tuller H L 1980 *J. Electrochem. Soc.* **127** 1969–73